materials

MDPI

Article

Testing Silica Fume-Based Concrete Composites under Chemical and Microbiological Sulfate Attacks

Adriana Estokova [1,*], Martina Kovalcikova [1], Alena Luptakova [2] and Maria Prascakova [2]

[1] Institute of Environmental Engineering, Faculty of Civil Engineering, Technical University of Kosice, Kosice 04200, Slovak Republic; martina.kovalcikova@tuke.sk

[2] Institute of Geotechnics, Slovak Academy of Sciences, Kosice 04001, Slovak Republic; luptakal@saske.sk (A.L.); prascak@saske.sk (M.P.)

* Correspondence: adriana.estokova@tuke.sk; Tel.: +421-55-602-4265

Academic Editor: Andreas Taubert

Received: 26 February 2016; Accepted: 21 April 2016; Published: 29 April 2016

Abstract: Current design practices based on descriptive approaches to concrete specification may not be appropriate for the management of aggressive environments. In this study, the durability of cement-based materials with and without the addition of silica fume, subjected to conditions that leach calcium and silicon, were investigated. Chemical corrosion was simulated by employing various H_2SO_4 and $MgSO_4$ solutions, and biological corrosion was simulated using *Acidithiobacillus* sp. bacterial inoculation, leading to disrupted and damaged surfaces; the samples' mass changes were studied following both chemical and biological attacks. Different leaching trends were observed via X-ray fluorescence when comparing chemical with biological leaching. Lower leaching rates were found for concrete samples fortified with silica fume than those without silica fume. X-ray diffraction and scanning electron microscopy confirmed a massive sulfate precipitate formation on the concrete surface due to bacterial exposure.

Keywords: concrete; corrosion; leaching; silica fume

1. Introduction

Concrete structures are generally considered to be durable because of their longer service life; however, they can deteriorate for a variety of reasons, including material limitations, poor quality design, and construction practices, as well as exposure to extreme environmental conditions [1]. Deterioration will occur when an environmental agent breaks the inorganic bonds of the cement binder. Acids, sulfates, NH_4^+ and Mg^{2+} salts, alkalis, organic esters, and CO_2 can destroy the binder over time [2,3].

Sulfate destruction of concrete occurs as a result of both chemical and physical processes [4,5]. Two main reactions are involved, namely, the reaction of SO_4^{2-} with hydrated calcium aluminates forming ettringite and the combination of SO_4^{2-} with free $Ca(OH)_2$ forming gypsum [6]. Considerable increases in volume are due to both reactions, causing the expansion and disruption of the hardened concrete. More recently, a third form of sulfate attack, known as thaumasite attack, has been discovered. Thaumasite is a calcium silicate sulfate-carbonate hydrate ($Ca_3Si(OH)_6(CO_3)(SO_4)\cdot 12H_2O$) that forms at temperatures below 15 °C by a reaction between cement paste hydrates, carbonates, and sulfate ions. Its formation reduces the cement paste to a soft mulch [7].

Concrete bio-deterioration is primarily due to the metabolic activity of sulfur-oxidizing bacteria (SOB) belonging to the *Acidithiobacillus* and *Thiobacillus* genera, *A. thiooxidans*, and sulfate-reducing bacteria (SRB) [8]. SRB metabolic activity leads to the production of H_2S, which is oxidized by SOB to H_2SO_4. Biogenic H_2S is the metabolic end product of sulfate-reducing bacteria living in anaerobic zones of soil, polluted water, and sewage. The presence of H_2S and H_2SO_4 usually induces the

corrosion of concrete sewer pipes that are inadequately ventilated and have low sewage flow [9,10]. The concentration of biogenic H_2SO_4 in concrete pore solutions may be as high as 10%, corresponding to a pH value of less than 1.0. In some cases, the pore solution has reached a pH as low as 0.6 because of microbiologically induced attacks, even at an initial alkalinity of pH 13 [11].

Supplementary cementitious materials, such as silica fume, ground granulated blast-furnace slag, and natural pozzolans, are added to concrete as part of the total cementitious system to improve the durability of concrete in an aggressive sulfate environment [12–15]. The addition of silica fume is assumed to improve the durability of concrete via a reduction in permeability, which refines pore structure, leading to the suppression of the diffusion of harmful ions, reducing $Ca(OH)_2$ content and, in turn, increasing resistance to sulfate attack [16–19]. Additionally, silica fume has been recognized as a pozzolanic admixture that is effective in enhancing mechanical properties to a great extent [20–22]. Silica fume, a mineral admixture composed of very fine solid glassy spheres of SiO_2, is a by-product of the smelting processes in the silicon and ferrosilicon industry [23]. Silica fume particles are extremely small, with more than 95% of the particles finer than 1 μm and generally 50- to 100-fold finer than average cement or fly ash particles [24]. When used in conjunction with Portland or blended cement, silica fume improves the microstructure of concrete by means of a microfilling ability and pozzolanic activity. During this process, waste is also transformed to reusable materials to help reduce industrial waste, thereby facilitating sustainable construction [25].

This study presents the results of different methods of analyzing the deterioration of silica-fume-based concrete due to the metabolic activity of sulfur-oxidizing bacteria and simulates an acidic and sulfate chemical corrosion. Various studies have focused on the investigation of silica fume-based concrete subjected only to chemical sulfate attack [26–28]. The significance of this research study lies in a comparison of both chemical and microbiological sulfate exposure, including the effect of the silica fume admixture used to improve concrete quality.

The objective of this study was, using X-ray fluorescence spectrometry (XRF), to examine the resistance of concrete composites with the addition of silica fume when considering the leaching of the primary cement matrix components Ca^{2+} and Si^{4+} due to sulfate exposure. The results are also analyzed in the context of the Si^{4+} and Ca^{2+} leaching rates, calculated by considering the maximum measured amount of Ca^{2+} (or Si^{4+}) in the leachates, and the mass changes of concrete samples after the experiment due to the formation of surface precipitates using scanning electron microscopy/energy dispersive X-ray microanalysis (scanning electron microscopy/energy dispersive X-ray microanalysis, SEM/EDX) and X-ray powder diffraction (XRD).

2. Results and Discussion

The major components of the concrete samples measured via XRF prior to the experiment are illustrated in Table 1 in oxide form.

Table 1. Chemical analysis of the analyzed concrete samples.

Mixture	Chemical Composition (wt %)												
	Na_2O	MgO	Al_2O_3	SiO_2	P_2O_5	SO_3	Cl	K_2O	CaO	TiO_2	MnO	Fe_2O_3	Other
M0	0.11	3.4	5.21	30.16	0.10	2.89	0.02	0.77	31.27	0.27	0.37	4.4	21.75
M1	0.11	2.73	5.39	45.63	0.09	2.72	0.02	0.79	26.17	0.26	0.36	3.75	11.98

Note: wt. %: weight percentage.

The M1 samples with the addition of silica fume (5 wt % of total binder mass) contained a higher percentage of SiO_2 (up to 45.63%) compared with the M0 samples (30.16%) without the addition of silica fume, as can be observed in Table 1. The difference in SiO_2 content was linked with the chemical composition of silica fume, which was composed of more than 90% SiO_2 (see Section 3.1). However, the percentage of CaO decreased in silica fume-based samples by 5% compared with samples without

silica fume. Only small differences in the concentrations of the other components were detected between the M0 and M1 concrete samples.

2.1. Chemical Leaching of Si^{4+} and Ca^{2+}

Different leaching trends were observed for the various media (Figure 1). The leaching of Si^{4+} and Ca^{2+} appears to increase with exposure duration (R = 0.98 and R = 0.89, respectively) for H_2SO_4 at pH 3.0 (M0-1) over 270 days; in other media, less Si was leached out over time. This was also naturally true for Ca^{2+} and is in accordance with the literature [29]. Regarding the media-leaching efficiency, the highest quantities of dissolved Si^{4+} and Ca^{2+} were measured in H_2SO_4 with a pH of 3.0, whereas the lowest concentrations were observed in fresh water throughout the experiment.

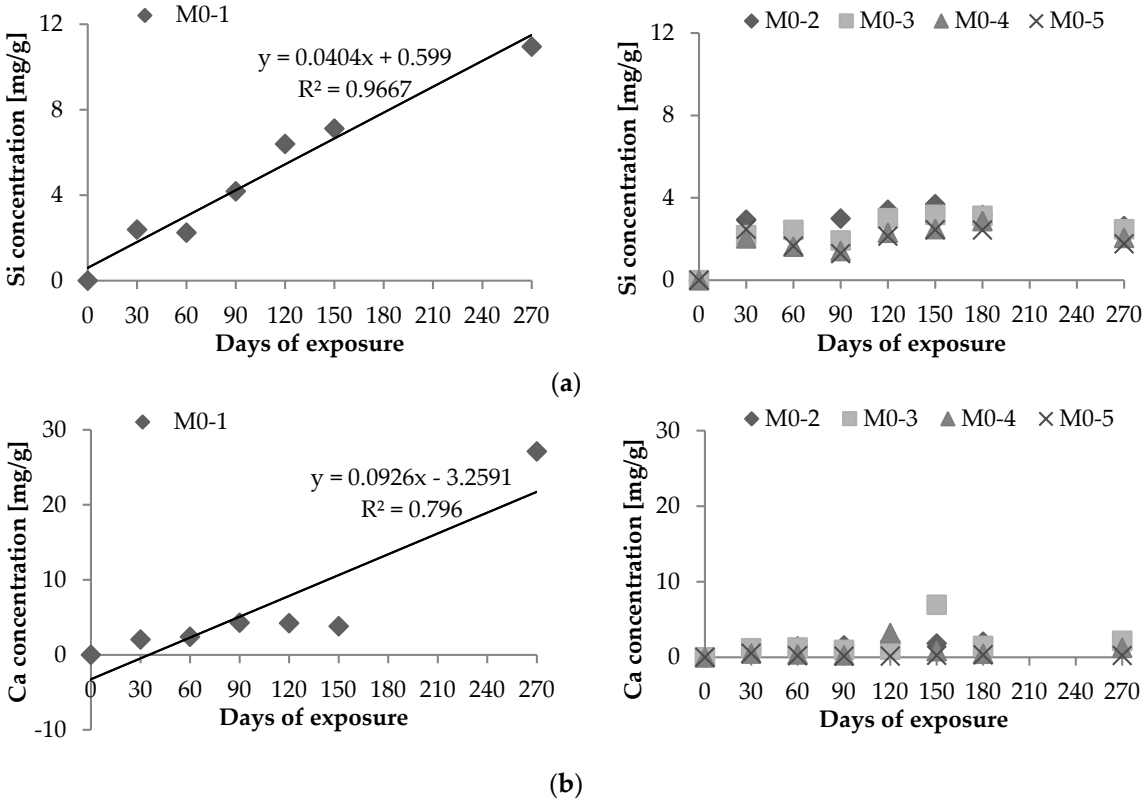

Figure 1. Dissolved: (**a**) Si^{4+} and (**b**) Ca^{2+} corresponding to 1 g of concrete samples without the addition of silica fume.

Si^{4+} and Ca^{2+} leaching trends of concrete samples with silica fume are illustrated in Figure 2 for various sulfate environments as well as fresh water. Quantities of dissolved Si^{4+} and Ca^{2+} correspond to 1 g of concrete samples.

The most intensive leaching of Si^{4+} (10.2 mg· g^{-1}) during the 270 days of exposure was observed for concrete sample M1-1 exposed to an aggressive environment of H_2SO_4 with a pH of 3 as observed in Figure 2a. The concentration of dissolved Si^{4+} in leachates was the lowest for sample M1-4 immersed in a solution of $MgSO_4$ with a concentration of SO_4^{2-} 3 g· L^{-1} (Figure 2a). Senhadji *et al.* [17] attributed the effect of silica fume on sulfate resistance more to chemical effects than reduced permeability while investigating the resistance of concrete to decomposition in $MgSO_4$ and Na_2SO_4 solutions. Zelic *et al.* mentioned that a silica fume replacement enhances the durability of mortar exposed to magnesium sulfate attack by lowering the lime content, thereby increasing the initial compressive strength; this occurs due to the pozzolanic reaction [30].

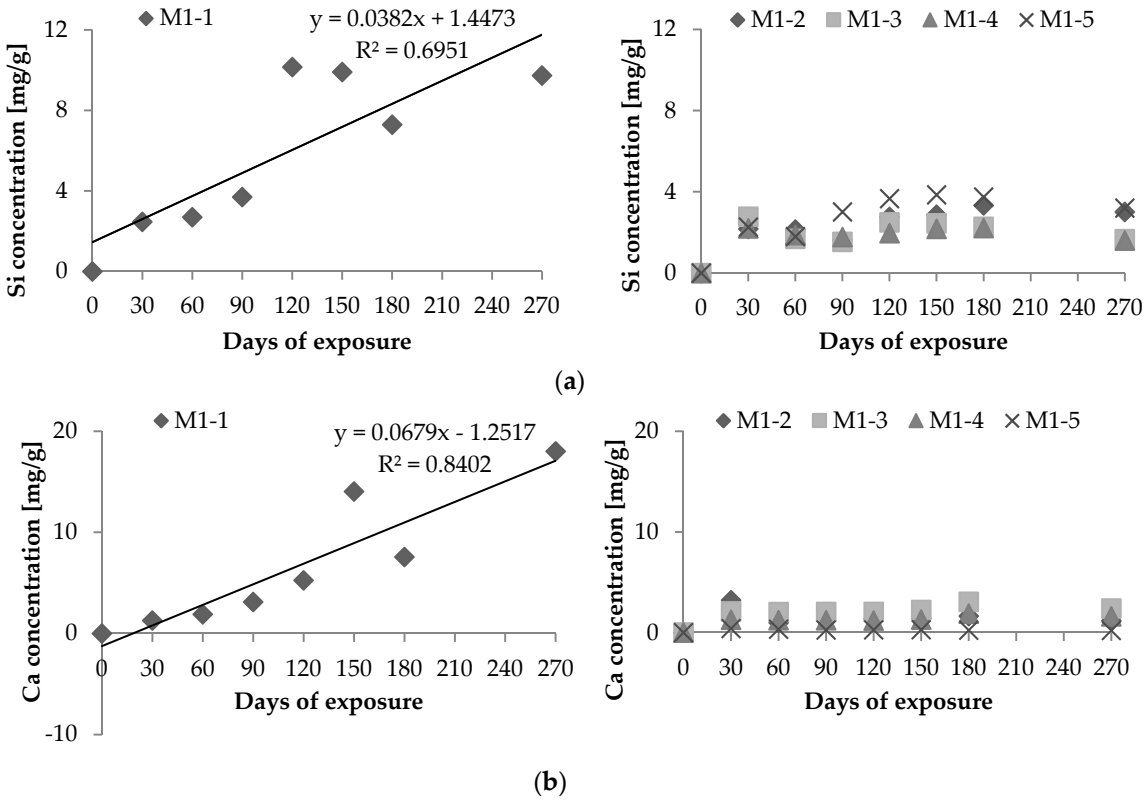

Figure 2. Dissolved: (**a**) Si^{4+} and (**b**) Ca^{2+} corresponding to 1 g of concrete samples with the addition of silica fume.

The maximum amount of dissolved Ca^{2+} (18.0 mg· g^{-1}) was observed in the leachate of sample M1-1 after 270-day experiments (Figure 2b). The concrete sample M1-5 exposed to fresh water was found to have the lowest values of leached-out Ca^{2+} during the experiment. Similar to concrete samples without silica fume, different leaching courses have been identified in concrete samples with silica fume. H_2SO_4 (pH 3) was confirmed to be the most aggressive towards concrete, exhibiting a linear correlation between the leached Si^{4+} and Ca^{2+} concentrations with R = 0.83 and 0.92 exposure times, respectively.

The leaching courses of the other media exhibited an increasing trend until 150 or 180 days of the exposure, after which leaching decreased. The lower concentrations of the Si^{4+} and Ca^{2+} in the leachates at the end of the experiment compared with the maximum at days 150 and 180, respectively, could be explained by the precipitation of newly formed compounds containing Ca^{2+} and Si^{4+} on the concrete surfaces as observed using X-ray powder diffraction (XRD). Traces of gypsum and quartz on the surface of concrete samples were also confirmed (Figure 3).

The similarity between leaching courses of Si^{4+} and Ca^{2+} for both silica fume- and non-silica fume-based concrete samples was confirmed for the media used in the chemical corrosion simulation.

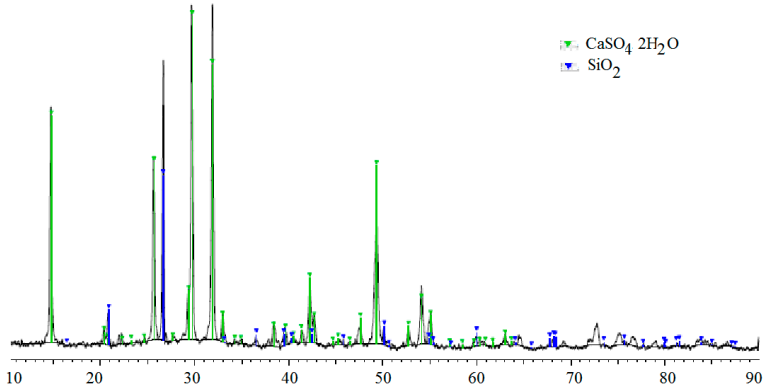

Figure 3. X-ray powder diffraction (XRD) diffractogram of the surface precipitates.

2.2. Biological Leaching of Ca^{2+} and Si^{4+}

Substantially more intensive Si^{4+} and Ca^{2+} leaching was found in the presence of *Acidithioxidans* bacteria (M0-6 and M0-7 samples) compared with fresh water (M0-5) than previously assumed (Figure 4).

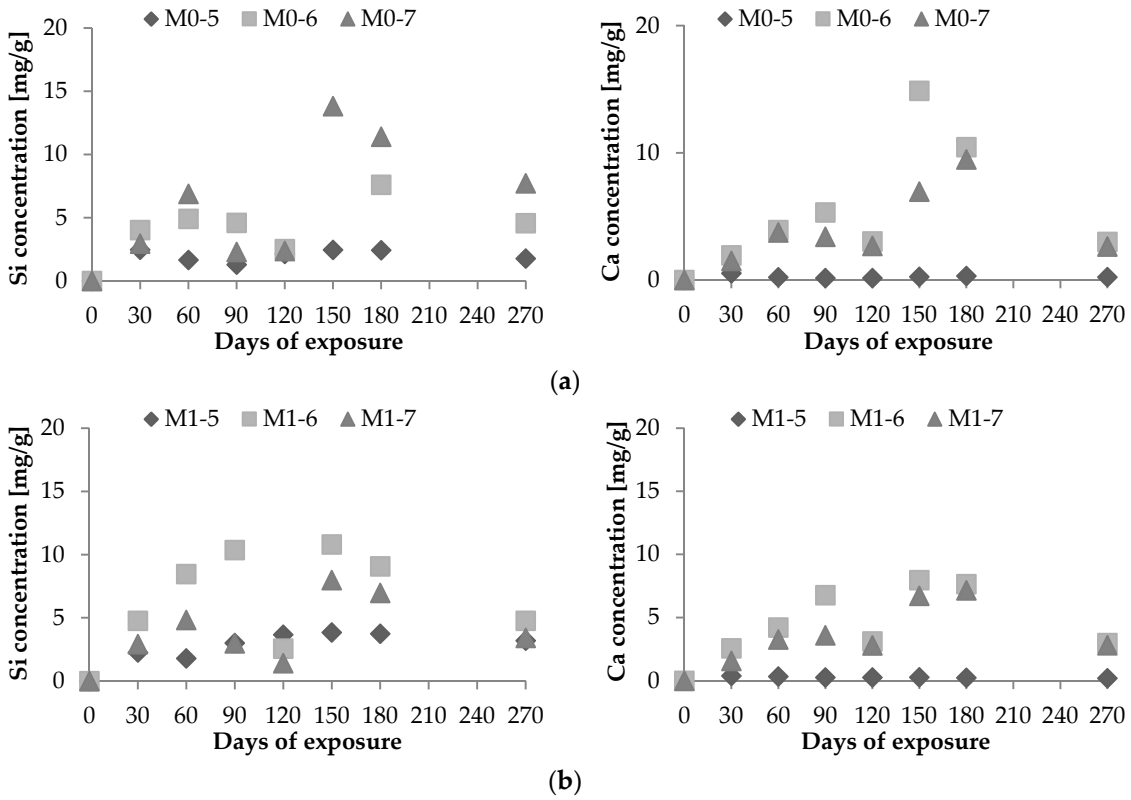

Figure 4. Dissolved Si^{4+} and Ca^{2+} corresponding to 1 g of concrete samples (**a**) without and (**b**) with the addition of silica fume.

No linear correlation between dissolved concentrations of Si^{4+} and Ca^{2+} and exposure time was observed. With the exception of the concentrations measured on day 120, it can be concluded that the concentrations of dissolved Si^{4+} and Ca^{2+} increased until day 150 of the bacterial exposure and thereafter significantly decreased. This can be related to the formation of massive sulfate precipitants on the surface of the concrete samples as reported in the study by Nielsen *et al.* [31]. The white covering of the samples under bacterial attack was more intensive compared with concrete samples subjected to

chemical attack. By decreasing the lime content in mortars during Mg-sulfate immersion, the formation of gypsum and ettringite, which are responsible for decreasing mortar durability, decreases [32].

2.3. Comparison of Chemical and Biological Corrosion

Figure 5 shows a comparison of quantities of leached Si^{4+} and Ca^{2+} due to both chemical and biological corrosion from samples made of two different mixtures after 270-day experiments corresponding to a 1-g concrete sample.

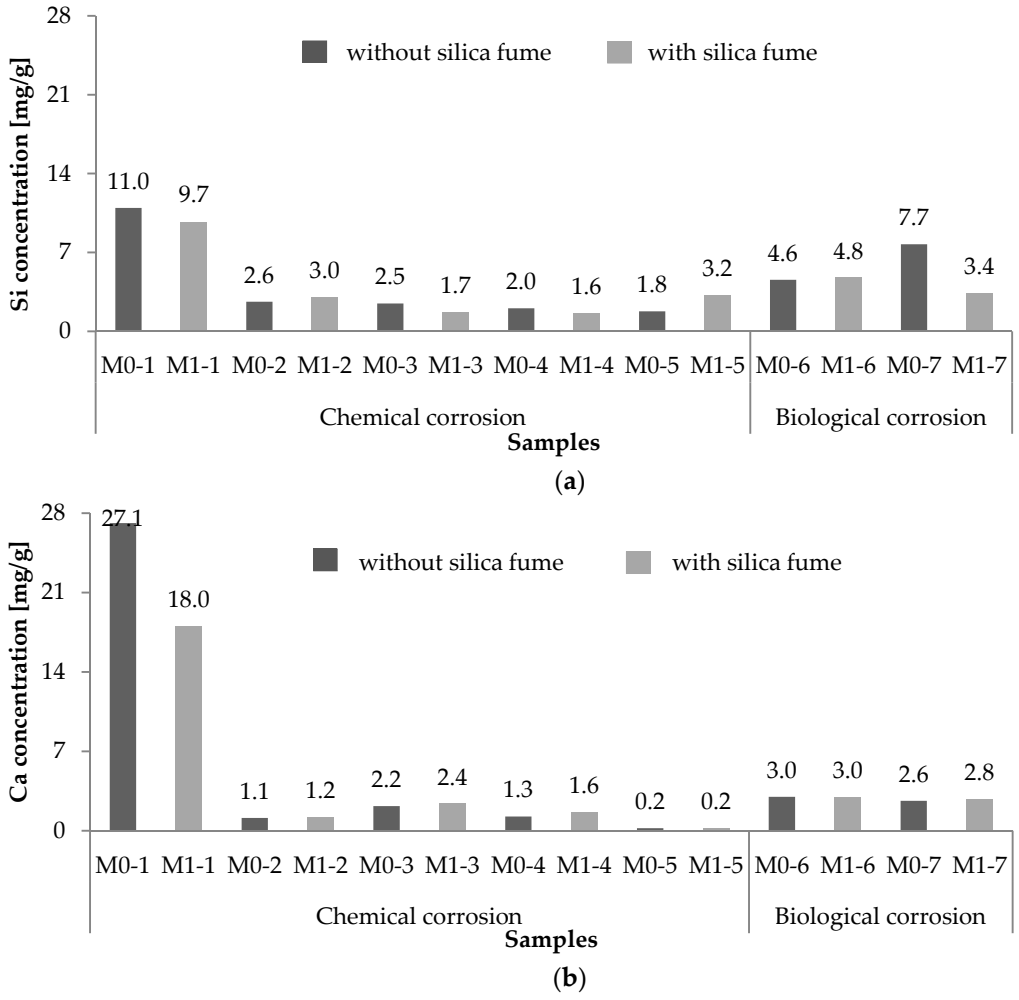

Figure 5. Leached-out masses of (**a**) Si and (**b**) Ca after the 270-day experiment.

By comparing two different mixtures of cement composites made of ordinary Portland cement without silica fume (M0) and with silica fume (M1), the concrete mixture with silica fume was found to be more durable, in terms of Si^{4+} leaching, when exposed to aggressive environments of H_2SO_4 with a pH of 3, both $MgSO_4$ solutions, and a diluted bacterial medium. However, lower durability, after the evaluation of Si^{4+} leaching, was detected in the H_2SO_4 with a pH of 4.0, concentrated bacterial medium, and fresh water.

When comparing the chemical and biological corrosion (Figure 5a), Si^{4+} leaching was more significant when subjected to bacterial exposure, with the exception of H_2SO_4 with a pH of 3 (M0-1 and M1-1 samples).

As for Ca^{2+} leaching, the concrete mixture with silica fume was found to be more durable in the aggressive environment of H_2SO_4 with a pH of 3, concentrated bacterial medium, and fresh water than in the other aggressive environments, as can be observed in Figure 5b. Based on the leached-out

masses of Ca^{2+} after the experiment, bacterial exposure was found to be the most significant compared with the chemical exposure with the exception of H_2SO_4 with a pH of 3. However, the Si^{4+} and Ca^{2+} concentrations at the end of the 270-day experiment likely do not represent the total amounts of dissolved ions. Therefore, the Si^{4+} and Ca^{2+} leaching rates were calculated by considering the maximum measured amount of Ca^{2+} (or Si^{4+}) in the leachates. The leaching rate V_d was calculated by dividing the measured mass of Si^{4+} or Ca^{2+} in a particular aggressive environment according to the corresponding time of exposure, as shown in Equation (1), based on the work of Ikeda *et al.* [33]:

$$V_d = \frac{X_d}{T \times S} \quad (1)$$

where

V_d: Si^{4+} (or Ca^{2+}) leaching rate per unit area ($\mu g \cdot h^{-1} \cdot cm^{-2}$);

X_d: maximum amount of Si^{4+} (or Ca^{2+}) leached out during the experiment (μg);

T: period of test [=24 × days of leaching (hours)]; and

S: area of exposure surface (cm^2).

Calculated Si^{4+} and Ca^{2+} leaching rates are reported in Table 2.

Table 2. The leaching rates of Si and Ca.

Samples without SF (M0)							
Element	**Chemical Corrosion**					**Biological Corrosion**	
	M0-1	M0-2	M0-3	M0-4	M0-5	M0-6	M0-7
	$V_{d\,max} \times 10^{-2}$ μg/(h × cm^2)						
Si	6.410	1.466	1.259	0.949	4.906	10.537	5.486
Ca	16.942	0.677	2.759	1.584	1.044	5.906	3.134
Samples with SF (M1)							
Element	**Chemical Corrosion**					**Biological Corrosion**	
	M1-1	M1-2	M1-3	M1-4	M1-5	M1-6	M1-7
	$V_{d\,max} \times 10^{-2}$ μg/(h × cm^2)						
Si	3.933	1.102	5.504	0.732	1.529	4.288	3.170
Ca	3.969	6.353	1.008	0.620	0.775	3.163	2.367

Lower leaching rates have been identified for concrete samples with the addition of silica fume (M1) as opposed to samples without silica fume (M0) in corresponding media (Table 2). As reported by Lee *et al.*, the incorporation of 10% silica fume in ordinary Portland cement matrix showed that the total reduction in strength was greater for mortar specimens without silica fume compared with those with silica fume [26]. Similarly, Ganjian and Pouya discovered that the performance of pastes and concrete specimens with silica fume exposed to simulation ponds and a site tidal zone were inferior to those without the silica fume replacement [34]. However, Hekal *et al.* reported that a partial replacement of Portland cement by silica fume (10%–15%) did not show a significant improvement in sulfate resistance of hardened cement pastes [35].

Higher rates of Si^{4+} than Ca^{2+} leaching were detected for all samples subjected to bacterial attack. A comparison of the Si^{4+} and Ca^{2+} leaching rates due to H_2SO_4 (pH 4) attack and a bacterial medium with the same pH of 4 revealed that the bacterial attack was more aggressive.

To confirm the superior performance of silica fume-based concrete in an aggressive sulfate environment, the mass percentage of the dissolved ions (Table 3) was also calculated. The percentage of dissolved ions was calculated by dividing the maximum quantity of dissolved ions by the total quantity of ions in concrete samples prior to the experiment.

Table 3. The wt % of dissolved Si and Ca.

Samples without SF (M0)							
Element	**Chemical Corrosion**					**Biological Corrosion**	
	M0-1	M0-2	M0-3	M0-4	M0-5	M0-6	M0-7
Si	13.75	2.61	2.25	2.04	1.76	26.29	31.63
Ca	22.21	0.89	3.02	1.38	0.23	6.45	13.26
Samples with SF (M1)							
Element	**Chemical Corrosion**					**Biological Corrosion**	
	M1-1	M1-2	M1-3	M1-4	M1-5	M1-6	M1-7
Si	4.76	1.56	1.30	1.04	1.81	5.07	9.60
Ca	9.62	1.71	1.63	1.00	0.21	4.26	9.82

The superior performance of concrete samples based on silica fume in terms of both Si^{4+} and Ca^{2+} leachability was confirmed for all concrete samples with the exception of samples immersed in fresh water. The most significant difference was noticed for samples subjected to bacterial attack. The calculated leachable fraction of Si^{4+} was 5.2- and 3.3-fold higher for samples without silica fume compared with the samples with silica fume after bacterial inoculation. Significantly lower leachable fractions of both Si^{4+} and Ca^{2+} ions were also observed for silica fume-based samples exposed to H_2SO_4 with a pH of 3 (2.9-fold for Si^{4+} and 2.3-fold for Ca^{2+}).

The results of the mass changes of the analyzed concrete samples prior to and after the experiments are given in Table 4.

Table 4. Changes in mass after the 270-day experiment.

Samples without SF (M0)							
Mass (g)	**Chemical Corrosion**					**Biological Corrosion**	
	M0-1	M0-2	M0-3	M0-4	M0-5	M0-6	M0-7
Before the experiment	69.61	69.81	73.19	81.96	83.47	76.91	74.73
After the experiment	68.10	69.28	73.10	81.61	82.68	77.56	75.76
Mass change (g)	1.51	0.53	0.09	0.35	0.79	−0.65	−1.03
Samples with SF (M1)							
Mass (g)	**Chemical Corrosion**					**Biological Corrosion**	
	M1-1	M1-2	M1-3	M1-4	M1-5	M1-6	M1-7
Before the experiment	75.61	83.36	84.49	95.41	96.77	81.31	93.10
After the experiment	73.78	81.85	83.73	94.08	95.19	82.01	94.35
Mass change (g)	1.83	1.51	0.76	1.33	1.58	−0.7	−1.25

A decrease in mass was noticed for all concrete specimens after the chemical corrosion experiments, whereas an increase in mass was detected for all samples after the biological corrosion experiments, as can be observed in Table 4. The increase in mass for all samples under bacterial exposure is likely a result of the formation of massive precipitants on the surfaces of the concrete.

A histogram of mass changes of the concrete specimens with and without the addition of silica fume prior to leaching and after 270 days of leaching is shown in Figure 6.

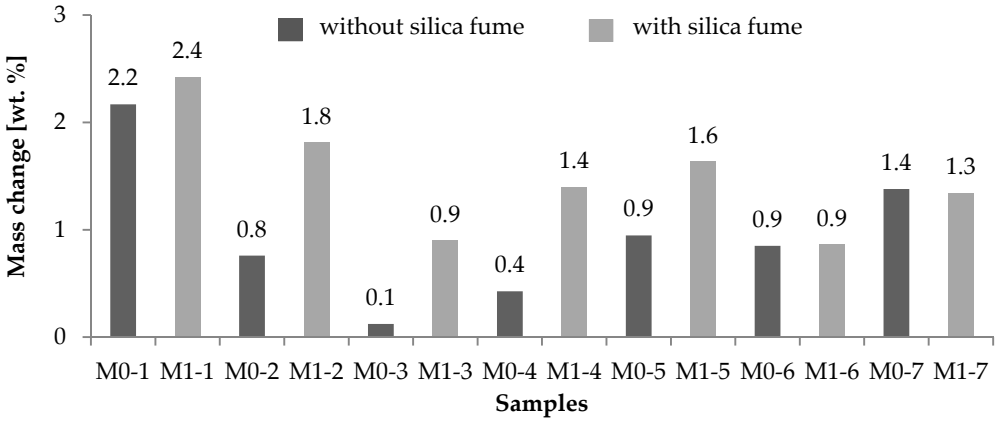

Figure 6. Mass changes of concrete samples.

The percentage of mass changes for concrete samples varied from 0.12% (sample M0-3) to 2.42% (sample M1-1). The highest decrease in concrete mass was detected for samples exposed to the most aggressive environment, represented by H_2SO_4 with a pH of 3, which corresponds with the findings regarding the leaching of Si^{4+} and Ca^{2+}. Surprisingly, higher mass changes were found for all concrete samples with the addition of silica fume than samples without silica fume. As is known, the deterioration of concrete can be caused by both mechanisms: (i) a dissolution of the cement paste constituents and its subsequent removal from the paste matrix due to its inherently high solubility and (ii) chemical reactions within the paste, e.g., salt crystallization, resulting in concrete volume expansion. The decrease in mass is linked with the leaching process, whereas an increase in mass can be linked with the penetration of sulfate solutions either by simple diffusion or capillary suction, which causes some salts to undergo cycles of dissolution and crystallization. The mass changes after chemical exposure indicate that the leaching process dominates in silica fume-based samples, whereas the crystallization process dominates in concrete samples without silica fume.

The formation of easily visible corrosion-induced cracks on the surface of concrete samples exposed to different aggressive media has been observed (Figures 7 and 8). No significant changes were identified in concrete samples M0-5 or M1-5 immersed in fresh water with a pH of 7.2.

(**a**) (**b**)

Figure 7. Samples (**a**) without and (**b**) with the addition of silica fume after the chemical exposure.

(**a**) (**b**)

Figure 8. Samples (**a**) without and (**b**) with the addition of silica fume after the bacterial exposure.

The surfaces of the concrete samples under chemical exposure contained only traces of precipitates, whereas the surface of the concrete samples under bacterial exposure was nearly completely covered by white crystalline compounds. The concrete samples with and without silica fume exposed to H_2SO_4 with a pH of 4 (M0-2 and M1-2 samples) and concentrated bacterial medium with a pH of 4 (M0-6 and M1-6 samples) were also analyzed using SEM and EDX, similar to our previous work [36]. The presence of the new surface products containing SO_4^{2-} (gypsum and thaumasite) was observed via SEM (Figure 9) and EDX (Figure 10).

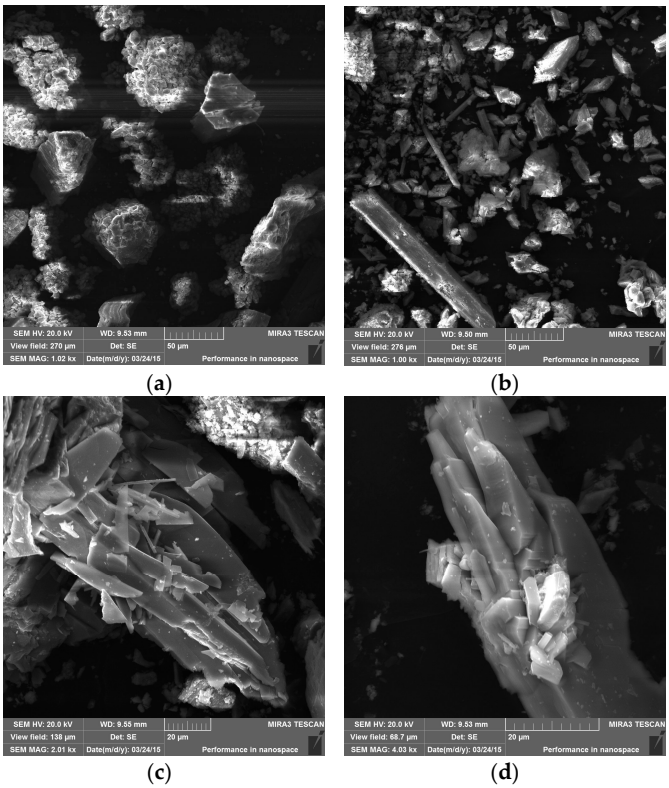

(**a**) (**b**)

(**c**) (**d**)

Figure 9. Scanning electron microscopy (SEM) micrographs of (**a**) M0-2; (**b**) M1-2; (**c**) M0-6; and (**d**) M1-6 samples.

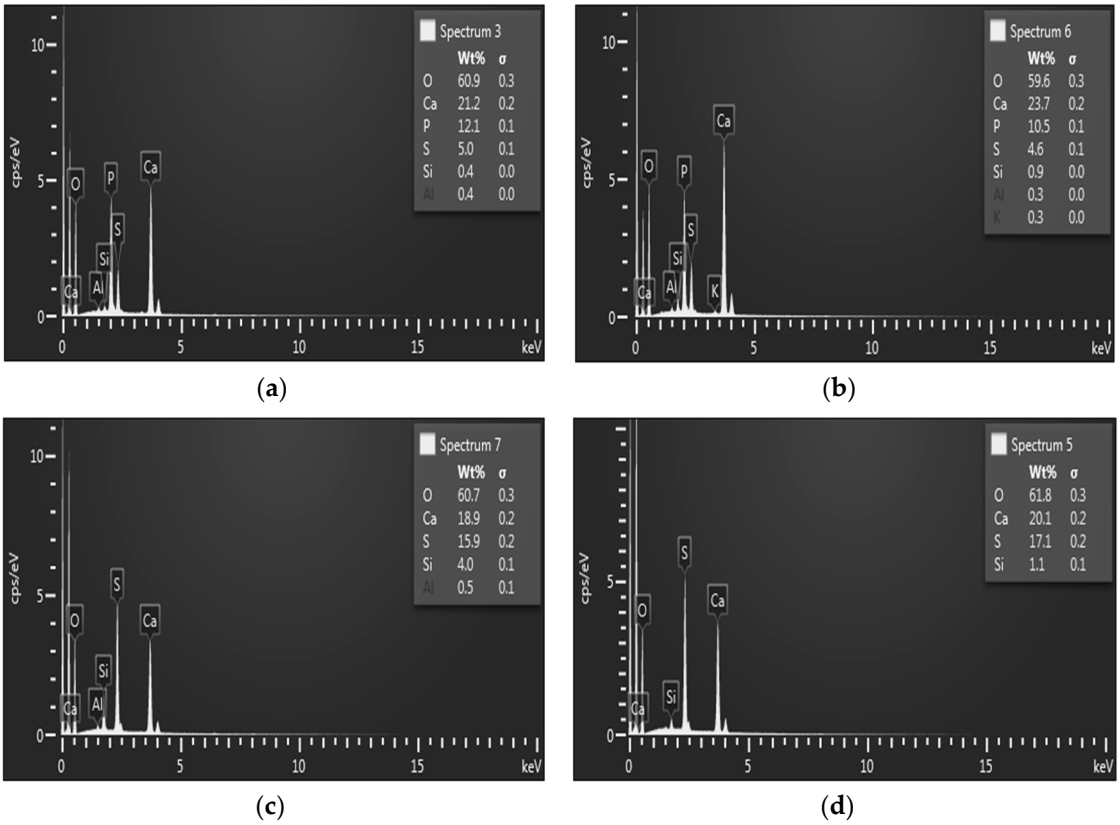

Figure 10. Energy dispersive X-ray microanalysis (EDX) semi-quantitative analysis of (**a**) M0-6; (**b**) M1-6; (**c**) M0-2; and (**d**) M1-2 samples.

The surface products observed were analyzed by EDX to confirm the presence of Ca^{2+} and Si^{4+} compounds (Figure 10).

As can be observed in Figure 10c,d, the presence of Ca, Si, O, and S in the surface compounds was confirmed. Based on the EDX and XRD analyses presented above, the presence of thaumasite ($Ca_3Si(OH)_6(CO_3)(SO_4)\cdot 12H_2O$) and gypsum ($CaSO_4\cdot 2H_2O$) can be assumed to be acting on the concrete surfaces. As reported by Schmidt *et al*. [37], despite the fact that thaumasite is thermodynamically favorable and more stable at lower temperatures, it can also be detected at 20 °C at low concentrations after sulfate interaction. Secondary gypsum forms parallel to thaumasite at high concentrations of SO_4^{2-}.

3. Materials and Methods

3.1. Cement and Silica Fume

The concrete samples used in the experiment were prepared using cement CEM I 42.5 N (Povazska cementaren, Ladce, Slovak Republic). The basic chemical composition of cement measured using XRF (SPECTRO iQ II, Spectro-Ametek, Kleve, Germany) in wt % was as follows: 1.37 MgO, 4.02 Al_2O_3, 18.11 SiO_2, 0.33 P_2O_5, 1.49 SO_3, 0.06 Cl, 1.12 K_2O, 57.15 CaO, 0.18 TiO_2, 0.001 MnO, and 2.70 Fe_2O_3. Basic components of silica fume (OFZ a.s., Istebne, Slovakia), representing a mineral waste admixture, measured using XRF in wt % were as follows: 1.07 MgO, 0.36 Al_2O_3, 92.46 SiO_2, 0.05 P_2O_5, 0.07 SO_3, 0.14 Cl, 0.99 K_2O, 0.23 CaO, 0.58 MnO, and 1.24 Fe_2O_3.

3.2. Concrete Composite Samples

Two mixtures (M0 and M1), per m^3, consisting of cement (Povazska cementaren), silica fume (OFZ a.s.), water, aggregate (Vychodoslovenske stavebne hmoty, Geca, Slovakia) with particle

size fractions of 0/4 mm, 4/8 mm, and 8/16 mm, and plasticizer Stachement 2353 based on polycarboxylates (Stachema, Bratislava, Slovakia) were employed (Table 5). According to the literature, the water demand of concrete containing silica fume increases with increasing amounts of silica fume.

Table 5. Composition of concrete mixtures (per m^3).

Component	M0	M1
Cement (kg/m^3)	360	360
Silica fume (kg/m^3)	-	20
Natural aggregates, fraction 0/4 mm (kg/m^3)	825	750
Natural aggregates, fraction 4/8 mm (kg/m^3)	235	235
Natural aggregates, fraction 8/16 mm (kg/m^3)	740	740
Water (L)	170	191
Polycarboxylate plasticizer (L)	3.1	3.1

Mixtures M0 and M1 were designed to meet the requirement of at least C30/37 concrete strength class and a water-cement ratio (w/c) of a maximum of 0.5 in accordance with EN 206-1. The concrete samples met the criteria for exposure class XA2 [38] with water to cement ratios of 0.47 (M0) and 0.49 (M1) and compressive strengths of 41.2 (M0) and 46.9 MPa (M1); their bulk densities were 2350 (M0) and 2380 $kg \cdot m^{-3}$ (M1). Slightly different water to cement ratios of M0 and M1 concrete mixtures were designed to maintain consistency (Slump S2) in the mixtures. Standardized concrete prisms measuring 100 × 100 × 400 mm^3 were poured and cured for 28 days immersed in water at the ambient temperature of 20 °C prior to testing [39,40]. The prisms were cut into smaller prisms measuring 50 × 50 × 10 mm^3 for corrosion testing. They were slightly brushed to remove loose particles, sterilized in 70% ethanol for 24 h to disinfect the concrete surfaces before the bacterial experiment, and dried at 105 °C until a constant mass was reached. Constant mass was achieved when less than 0.1% of the test sample wet mass is lost during additional exposure to the drying process.

3.3. Chemical Corrosion Simulation

The latter concrete prisms were exposed by immersion into 400 mL of 0.005 wt % H_2SO_4, pH 3.0 (samples: M0-1, M1-1), and 0.0005 wt % H_2SO_4, pH 4.0 (samples: M0-2, M1-2), in glass beakers, both being daily checked for pH (FG2-FiveGo, Mettler-Toledo, Switzerland) and kept constant by the addition of 0.1 M H_2SO_4. Other prisms were immersed into 400 mL of $MgSO_4$ solution of 12.5 $g \cdot L^{-1}$ with SO_4^{2-} 10 $g \cdot L^{-1}$ (samples M0-3 and M1-3), an $MgSO_4$ solution of 3.75 $g \cdot L^{-1}$ with SO_4^{2-} 3 $g \cdot L^{-1}$ (samples M0-4 and M1-4), and fresh water with a pH of 7.2 (samples M0-5 and M1-5) for concrete corrosion resistance testing [38]. The volume of the liquid media was based on the volume ratio of the concrete prisms and liquid phase (S/L) 1:10. Leaching durations were set at intervals of 30, 60, 90, 120, 150, 180, and 270 days at a temperature of 23 °C. After each 30-day period, the pH and the concentrations of the dissolved Ca^{2+} and Si^{4+} were measured in leaching media.

3.4. Microbial Corrosion Simulation

A culture of *A. thiooxidans* was isolated from an acid mine drainage (Pech shaft in the locality of Smolnik, Eastern Slovakia) as described by Waksman and Joffe [41].

The concrete prisms were exposed at 23 °C in covered glass jars to 400 mL of a bacterial culture medium consisting of 20 vol. % of bacterial inoculum and 80 vol % nutrient medium with pH 4.0 according to Waksman and Joffe (samples M0-6 and M1-6) or the same medium diluted with distilled water 1:1 (samples M0-7 and M1-7). Six milliliters of bacterial culture was inoculated at 7-day intervals over a period of 270 days. The concentrations of dissolved Si^{4+} and Ca^{2+} were measured in the leachates every 30 days.

3.5. Analytical Methods

The concentrations of Ca and Si in the leachates were determined using XRF (SPECTRO iQ II, Spectro-Ametek, Kleve, Germany) and a silicon drift detector with a resolution of 145 eV at 10,000 pulses. The primary beam was polarized with a Bragg crystal and highly ordered pyrolytic graphite target. Measurements were performed for 300 and 180 s at voltages of 25 kV and 50 kV and currents of 0.5 and 1.0 mA in the presence of helium.

To determine the chemical composition prior to and after the experiments, cement composites were crushed into powder (MSK-SFM-1 Desk-Top planetary ball mill, MTI Corporation, Richmond, VA, USA), and 5 g was mixed with 1 g of a dilution material (Hoechst wax C micropowder, Merck Millipore, Darmstadt, Germany) and subsequently pressed into a pellet at a pressure of 0.1 MPa$\cdot$ m^{-2}; this was analyzed using XRF.

The precipitates on the surface of the concrete samples after the experiments were removed and placed on adhesive carbon tape and studied using SEM/EDX (MIRA3 FE, Tescan, Brno, Czech Republic/Oxford Instruments, Abingdon, UK) and XRD (D2 PHASER diffractometer, Bruker, Germany) with Cu K_α radiation generated at 10 mA and 30 kV with a step size of 0.04° over the range 2θ from 10° to 90°.

4. Conclusions

This paper presents the results of a study on the deterioration of concrete samples caused by chemical and microbiological attacks. Attention was paid to the leachability of the most important components of the cement matrix: Si(IV) and Ca(II) compounds. The mass and surface changes due to this deterioration were of interest as well. The following conclusions have been obtained:

1. Microbiological attack precipitated by *Acidithiobacillus thiooxidans* was more dangerous, in terms of leaching of the main components, than chemical sulfate attack with the exception of a H_2SO_4 solution of a pH of 3.
2. The concrete samples equipped with silica fume exhibited better durability, in terms of the leaching of Si^{4+} and Ca^{2+}, than concrete samples without silica fume.
3. Significantly lower leachable fractions, specifically those 2.9- and 2.3-fold lower for Si^{4+} and Ca^{2+}, respectively, were observed for silica fume-based samples exposed to H_2SO_4 with a pH of 3 compared with samples without silica fume.
4. The calculated leachable fraction of Si^{4+} was 5.2- and 3.3-fold higher for samples without silica fume compared with the samples with silica fume under biological exposure.
5. Silica fume concrete is not impervious to all aggressive chemicals. However, the study shows that at a low water to cement ratio (w/c), silica fume concrete can effectively prevent significant damage following many types of chemical attack including sewage leachate. Based on this finding, silica fume concrete has been specified for use in sewer and outfall pipes.

Notably, many problems related to both the chemical and microbial corrosion of concrete have not been solved up to now despite considerable progress in the recognition of corrosion kinetics and mechanisms. Thus, further research on corrosion processes and methods of protection against these processes is necessary.

Acknowledgments: This research was carried out under grants No. 2/0145/15 and 1/0481/13 of the Slovak Grant Agency for Science.

Author Contributions: Adriana Estokova initiated the overall research concept, completed the initial manuscript, and critically revised the content of the paper. Martina Kovalcikova managed the experimental work, performed X-ray fluorescence spectrometry measurements, contributed to manuscript writing, and has been involved in revising the manuscript. Alena Luptakova carried out the biological corrosion experiments, analysed the data and partially interpreted it. Maria Prascakova characterized surface precipitates using SEM micrographs.

Conflicts of Interest: The authors declare no conflict of interest.

References

1. Shinkafi, S.A.; Haruna, I. Microorganisms associated with deteriorated desurface painted concrete buildings within Sokoto, Nigeria. *Int. J. Curr. Microbiol. Appl. Sci.* **2013**, *2*, 314–324.
2. Fleming, E. *Construction Technology: An Illustrated Introduction*; Blackwell Publishing: Oxford, UK, 2005; p. 380.
3. Little, B.J.; Lee, J.S. *Microbiologically Influenced Corrosion*; John Wiley & Sons: Hoboken, NJ, USA, 2007.
4. Tian, B.; Cohen, M.D. Does gypsum formation during sulfate attack on concrete lead to expansion? *Cem. Concr. Res.* **2000**, *30*, 117–123. [CrossRef]
5. Bellmann, F.; Stark, J. Prevention of thaumasite formation in concrete exposed to sulphate attack. *Cem. Concr. Res.* **2007**, *37*, 1215–1222. [CrossRef]
6. Ann, K.Y.; Cho, C.H.G. Corrosion resistance of calcium aluminate cement concrete exposed to a chloride environment. *Materials* **2014**, *7*, 887–898. [CrossRef]
7. King, D. The effect of silica fume on the properties of concrete as defined in concrete society report 74. In Proceedings of the 37th Conference on Our World in Concrete & Structures, Singapore, Singapore, 29–31 August 2012.
8. Wells, T.; Melchers, R.E. Modelling concrete deterioration in sewers using theory and field oservations. *Cem. Concr. Res.* **2015**, *77*, 82–96. [CrossRef]
9. Wei, S.; Jiang, Z.; Liu, H.; Zhou, D.; Sanchez-Silva, M. Microbiologically induced deterioration of concrete—A review. *Braz. J. Microbiol.* **2013**, *44*, 1001–1007. [CrossRef] [PubMed]
10. Wells, T.; Melchers, R.E. An observation-based model for corrosion of concrete sewers under aggressive conditions. *Cem. Concr. Res.* **2014**, *61–62*, 1–10. [CrossRef]
11. Cwalina, B. Biodeterioration of concrete. *ACEE* **2008**, *4*, 133–140.
12. Chen, M.C.; Wang, K.; Xie, L. Deterioration mechanism of cementitious materials under acid rain attack. *Eng. Fail. Anal.* **2013**, *27*, 272–285. [CrossRef]
13. Cyr, M. Influence of supplementary cementitious materials (SCMs) on concrete durability. In *Eco-Efficient Concrete*; Pacheco-Torgal, F., Jalali, S., Labrincha, J., John, V.M., Eds.; Woodhead Publishing: Oxford, UK, 2013.
14. Cheng, A.; Chao, S.J.; Lin, W.T. Effects of leaching behavior of calcium ions on compression and durability of cement-based materials with mineral admixtures. *Materials* **2013**, *6*, 1851–1872. [CrossRef]
15. Glinicki, M.A.; Jóźwiak-Niedźwiedzka, D.; Gibas, K.; Dąbrowski, M. Influence of Blended Cements with Calcareous Fly Ash on Chloride Ion Migration and Carbonation Resistance of Concrete for Durable Structures. *Materials* **2016**, *9*, 18. [CrossRef]
16. Torii, K.; Kawamara, M. Effects of fly ash and silica fume on the resistance of mortar to sulfuric acid and sulfate attack. *Cem. Concr. Res.* **1994**, *24*, 361–370. [CrossRef]
17. Senhadji, Y.; Escadeillas, G.; Mouli, M.; Khelafi, H.; Benosman, A.S. Influence of natural pozzolan, silica fume and limestone fine on strength, acid resistance and microstructure of mortar. *Powder Technol.* **2014**, *254*, 314–323. [CrossRef]
18. Estokova, A.; Kovalcikova, M.; Luptakova, A. Deterioration of cement composites with silica fume addition due to chemical and biogenic corrosive processes. *Solid State Phenom.* **2015**, *227*, 190–193. [CrossRef]
19. Nili, M.; Ehsanil, A. Investigating the effect of the cement paste and transition zone on strength development of concrete containing nanosilica and silica fume. *Mater. Des.* **2015**, *75*, 174–183. [CrossRef]
20. El Sokkary, T.M.; Assal, H.H.; Kandeel, A.M. Effect of silica fume or granulated slag on sulphate attack of ordinary Portland and alumina cement blend. *Ceram. Int.* **2004**, *30*, 133–138. [CrossRef]
21. Małolepszy, J.; Grabowska, E. Sulphate attack resistance of cement with zeolite additive. *Procedia Eng.* **2015**, *108*, 170–176. [CrossRef]
22. Sanjuán, M.A.; Argiz, C.; Gálvez, J.C.; Moragues, A. Effect of silica fume fineness on the improvement of portland cement strength performance. *Constructr. Build. Mater.* **2015**, *96*, 55–64. [CrossRef]
23. Saraya, M.E.I. Study physico-chemical properties of blended cements containing fixed amount of silica fume, blast furnace slag, basalt and limestone, a comparative study. *Constructr. Build. Mater.* **2014**, *72*, 104–112. [CrossRef]
24. Elsayed, A.A. Influence of silica fume, fly ash, super pozz, and high slag cement on water permeability and strength of concrete. *Concr. Res. Lett.* **2012**, *3*, 528–540.

25. Suhendro, B. Toward green concrete for better sustainable environment. *Procedia Eng.* **2014**, *95*, 305–320. [CrossRef]
26. Lee, S.T.; Moon, H.Y.; Swamy, R.N. Sulfate attack and role of silica fume in resisting strength loss. *Cem. Concr. Compos.* **2005**, *27*, 65–76. [CrossRef]
27. Chahal, N.; Siddique, R.; Rajor, A. Influence of bacteria on the compressive strength, water absorption and rapid chloride permeability of concrete incorporating silica fume. *Constr. Build. Mater.* **2012**, *37*, 645–651. [CrossRef]
28. Nehdi, M.L.; Suleiman, A.R.; Soliman, A.M. investigation of concrete exposed to dual sulfate attack. *Cem. Concr. Res.* **2014**, *64*, 42–53. [CrossRef]
29. Jooss, M. Leaching of concrete under thermal influence. *Otto Graf J.* **2001**, *12*, 51–68.
30. Zelic, J.; Radovanovic, I.; Jozic, D. The effect of silica fume additions on the durability of Portland cement mortars exposed to magnesium sulfate attack. *Mater. Technol.* **2007**, *41*, 91–94.
31. Nielsen, P.; Sven, N.; Darimont, A. Influence of cement and aggregate type on thaumasite formation in concrete. *Cem. Concr. Res.* **2014**, *53*, 115–126. [CrossRef]
32. Davis, J.L.; Nica, D.; Shields, K.; Roberts, D.J. Analysis of concrete from corroded sewer pipe. *Int. Biodeterior. Biodegrad.* **1998**, *42*, 75–84. [CrossRef]
33. Ikeda, M.; Otsuki, N.; Nishida, T.; Minagawa, H. Influence of type of cement on Ca leaching from concrete using experimental acceleration method. In Proceedings of the 29th Conference on Our World in Concrete & Structures, Singapore, 25–26 August 2004.
34. Ganjian, E.; Pouya, H.S. Effect of magnesium and sulfate ions on durability of silica fume blended mixes exposed to the seawater tidal zone. *Cem. Concr. Res.* **2005**, *35*, 1332–1343. [CrossRef]
35. Hekal, E.E.; Kishar, E.; Mostafa, H. Magnesium sulfate attack on hardened blended cement pastes under different circumstances. *Cem. Concr. Res.* **2002**, *32*, 1421–1427. [CrossRef]
36. Estokova, A.; Ondrejka Harbulakova, V.; Luptakova, A.; Prascakova, M.; Stevulova, N. Sulphur oxidizing bacteria as the causative factor of biocorrosion of concrete. *Chem. Eng. Trans.* **2011**, *24*, 1–6.
37. Schmidt, T.; Lothenbach, B.; Scrivener, K.L.; Romer, M.; Rentsch, D.; Figi, R. A thermodynamic and experimental study of the conditions of thaumasite formation. *Cem. Concr. Res.* **2008**, *38*, 337–349. [CrossRef]
38. European Committee for Standardization. *EN 206–1: 2002 Concrete. Specification, Performance, Production and Conformity*; European Committee for Standardization: Brussels, Belgium, 2002.
39. European Committee for Standardization. *EN 12390–1: 2013 Testing Hardened Concrete. Part. 1: Shape, Dimensions and other Requirements for Specimens and Moulds*; European Committee for Standardization: Brussels, Belgium, 2011.
40. European Committee for Standardization. *EN 12390–5: 2013 Testing Hardened Concrete. Part. 5: Flexural Strength of Test. Specimens*; European Committee for Standardization: Brussels, Belgium, 2011.
41. Karavajko, G.I.; Rossi, G.; Agate, A.D.; Groudev, S.N.; Avakyan, Z.A. *Biogeotechnology of Metals: Manual*; Centre for International Projects, GKNT: Moscow, Russia, 1998.